Taylor & Francis
Taylor & Francis Group

Molecular Crystals and Liquid Crystals

ISSN: 1542-1406 (Print) 1563-5287 (Online) Journal homepage: http://www.tandfonline.com/loi/gmcl20

The effect of graphite functionalization on electrical and shielding properties of epoxy composites

Oleksandra Lazarenko, Ludmila Vovchenko, Yulia Perets, Olena Yakovenko, Iryna Ovsiienko, Viktor Oliynyk, Mykola Melnychenko & Ludmila Matzui

To cite this article: Oleksandra Lazarenko, Ludmila Vovchenko, Yulia Perets, Olena Yakovenko, Iryna Ovsiienko, Viktor Oliynyk, Mykola Melnychenko & Ludmila Matzui (2016) The effect of graphite functionalization on electrical and shielding properties of epoxy composites, Molecular Crystals and Liquid Crystals, 639:1, 94-104, DOI: 10.1080/15421406.2016.1255032

To link to this article: http://dx.doi.org/10.1080/15421406.2016.1255032

MOLECULAR CRYSTALS AND LIQUID CRYSTALS
2016, VOL. 639, 94–104
http://dx.doi.org/10.1080/15421406.2016.1255032

Taylor & Francis
Taylor & Francis Group

The effect of graphite functionalization on electrical and shielding properties of epoxy composites

Oleksandra Lazarenko, Ludmila Vovchenko, Yulia Perets, Olena Yakovenko, Iryna Ovsiienko, Viktor Oliynyk, Mykola Melnychenko, and Ludmila Matzui

Department of Physics and Department of Radiophysics, Electronics and Computer Systems, Taras Shevchenko National University of Kyiv, Kyiv, Ukraine

ABSTRACT

Composite materials (CMs) based on epoxy resin and functionalized thermoexfoliated graphite (TEG) were prepared. The composition of functional groups at the TEG surface was characterized by FTIR spectroscopy. It was found that some of CMs with pristine TEG have high shielding efficiency in the region of electromagnetic radiation frequency from 25.5 to 37.5 GHz. But the main disadvantage of these CMs is their high porosity and heterogeneity that makes impossible to obtain the stable shielding characteristics for thin sample. However, CMs contained functionalized TEG are sufficiently homogeneous and allow purposefully regulate their electrical and shielding properties by changing TEG content.

KEYWORDS

Nanostructures; polymers; functionalization; electrical conductivity; shielding efficiency

Introduction

Currently because of the rapid development of technology, and wide applications of computer equipment, radiophones, communication, the problem regarding environmental safety needed to be solved urgently. In order to avoid the mentioned detrimental effects of electronic devices on living matter, the protective shield with high absorption of the microwave electromagnetic radiation (EMR) has been created. The composite materials (CMs) based on the polymer matrix and carbon nanofiller are commonly used for shielding against the EMR, owing to the unique electrophysical properties of nanocarbon and providing lightweight shielding materials. Conventionally, carbon nanotubes (CNT) are extremely interesting for conductive applications. CNT provide very low percolation threshold in CNT based composites and huge effective permittivity and electrical conductivity values [1, 2]. However, few-layered graphene sheets are also of great interest. Today, researchers are actively looking for graphene/polymer nanocomposites which promise to deliver strong, durable, and multifunctional materials with low nanofiller contents [3].

Graphite nanoplatelets (GNPs) are carbon nanostructures consisting of small stacks of graphene sheets with overall thickness from 1 nm to a few tens of nanometers, and lateral linear dimensions from a few micrometers up to hundreds of micrometers. De Bellis et al. [4] have shown that the GNP-filled composite have better shielding performances than the CNT-based ones due to the relatively higher effective conductivity. Due to their bi-dimensional

CONTACT Oleksandra Lazarenko alazar@univ.kiev.ua
Color versions of one or more of the figures in the article can be found online at www.tandfonline.com/gmcl.

shape, GNPs can play the role of the nano-filler with a high aspect ratio and, at the same time, can efficiently replace the micro-filler having the function of increasing the real part of the effective permittivity of the composite. Despite the great application potential, it is should be noted that graphene itself possesses zero band gap as well as inertness to reaction, which weakens the competitive strength of graphene in the field of semiconductors and sensors [5]. The nanocarbon particles in all forms tend to aggregation (nanographite, graphene-like structures), formation of bundles, tangled nets (CNTs, carbon nanofibers) due to relatively strong long-range Van der Waals interaction. One of the major challenges in the fabricating CM with desired properties is obtaining a uniform distribution of filler in the bulk of a polymer matrix as well as strong polymer-filler bonding.

Such problems as phase separation, filler particle agglomeration, non-uniform distribution in polymer matrix and weak matrix–filler adhesion could be solved through application of modern technologies of multifunctional treatment of nano-filler surface that optimize the interaction between filler and matrix. The uniform distribution of nanocarbon particles in polymer matrix is achieved by methods of mechanical and chemical treatment of nanocarbon component. During mechanical treatment of nanocarbon (ultrasonic dispersion, shaking, etc.) the physical separation of nanocarbon particles is occurring. When nanocarbon interacts with some substances (for example, oxygen, fluorine, ozone, oxyacids and some of oxygenic salts) the opening of CNTs, oxidation with formation of adsorbed or gaseous CO and CO_2 and joining functional groups to nanocarbon surface (nanocarbon surface functionalization) are occurring. As a result the properties of nanocarbon surface change. The functionalization of nanocarbon surface creates favourable conditions for uniform distribution of nanocarbon filler in polymer matrix and provides the strong connection between filler particles and polymer matrix [6]. There are the covalent and noncovalent functionalizations. Generally, covalent functionalization compromises the sp^2 structure of graphene lattices, thus resulting in defects and loss of the electronic properties [7]. In contrast, noncovalent functionalization is largely preferred as it does not alter the structure and electronic properties of graphene while it simultaneously introduces new chemical groups on the surface [8]. The alternative to the wet oxidation by acids is dry oxidation by UV/ozone treatment of nanocarbon particles [9]. Ozone is easily generated by exciting molecular oxygen with UV [10], and, as shown in [11], UV/ozone treatment is able to improve both the electrical conductivity and mechanical properties of NCs by improving GNPs/epoxy interfacial adhesion.

The aim of this investigation was to study the connection between functionalization method and structural and morphological parameters of functionalized nanocarbon and electrical and shielding properties of epoxy based composites.

Experimental and sample characterization

Thermoexfoliated graphite (TEG) prepared by acid intercalation of graphite was used as pristine material. Upon a rapid heating, the intercalated graphite was expanded explosively several hundred times along the thickness direction due to evaporation of intercalant. Pristine TEG was a high-porosity powder (packing density ~0.03 kg/m^3) with a highly developed active surface. It consisted of 1–3 mm particles of cellular structure, the size of cells (pores) is 5–10 μm, in this case the thickness of the cell walls does not exceed 100 nm [12]. It was functionalized using the several methods listed in Table 1.

Evidently, methods 1,2 are the methods of covalent functionalization, in which the mixtures of strong inorganic acids (2) or solution of strong oxidizing agent (potassium permanganate) in sulfur acid (1) are used as functionalization

Table 1. Methods of functionalization of TEG.

Name	Stages of TEG treatment for functionalization
GNPs1	1. Preparing of suspension of TEG powder in mixture of concentrated H_2SO_4 and HNO_3 (40 ml) (volume ratio is 1:3) Dispersion of suspension in magnetic stirrer for 1 hr. 2. Impregnation for 24 hrs. 3. Repeated dispersion of suspension in magnetic stirrer for 1–20 hrs. 4. Removing excess of acids by centrifugation (18514 g) for 1 hr. 5. Washing with distilled deionized water to remove sediment until pH neutral. 6. Drying of powder at 390K until constant mass (8 hrs).
GNPs2	1. Mixing of TEG powder with solution of $KMnO_4$(1.5M) in H_2SO_4 in magnetic mixer (1 h). 2. Boiling the mixture TEG in solution during 5 h and impregnationduring 24 h. 100 ml TEG – 200 ml of acids mixture. 3. Impregnationof TEG during 24 h. 4. Repeated mixing in magnetic mixer (1 h). 5. Filtration and washing in normal HCl acid. 6. Washing in distilleddeionized water. 7. Drying at 120°C to a steady mass.
GNPs3	1. Mixing of TEG powder with etanol in magnetic mixer (1 h) and impregnation during 24 h. 2. Repeated mixing in magnetic mixer (1 h). 3. Filtration and washing in distilleddeionized water. 4. Drying at 120°C to a steady mass.
GNPs4	1. Preparing of suspension TEG in acetone. 2. Dispersion of suspension in ultrasound of 50 W and 40 kHz for 3 hours in acetone. 3. Drying at 120°C to a steady mass.
GNPs4-UV	1. Preparing of suspension TEG in acetone. 2. Dispersion of suspension in ultrasound of 50 W and 40 kHz for 3 hours in acetone. 3. Drying at 120°C to a steady mass. 4. UV/ozone treatment for 20 min.

substance. Organic compounds liable to absorbing are used in the methods 3,4 of TEG functionalization.

The resulting GNPs were labeled as indicated in column 1 (Table 1). In case of ultrasonication in acetone (GNPs4) the GNP powders were divided in two parts. One part was subjected to UV/ozone treatment for 30 min, while the other was left intact. UV/ozone treatment was performed by DRT-1000 equipped with electric-discharge arc lamp of high pressure inflated with mercury and argon compound that could release ultraviolet radiation of 50W at 240–320 nm wave-length. The distance between the UV lamp and the sample stage was fixed at 11 cm.

Raman spectroscopy was carried out using a Horiba spectrometer LabRam at 532 nm equipped with a CCD camera. The X-ray diffraction investigations were performed using DRON-4–07 X-ray diffractometer (Co K_α filtered radiation), the wavelength $\lambda = 1.7902$A, exposition time was equal to 6 sec. The interplanar distance d_{002} was determined from the Braggs' equation. The size of the coherent scattering region (it is the size of crystallite in our case) is related with the half-width B by the following equation: $L_c = \frac{k_c\lambda}{\beta\cos(\theta)}$, $\beta = \sqrt{B^2 - b^2}$, where k_c is the form-factor of the reflection, $k_c = 0.89$, $b = 0.00239$ radian is the half-width of the standard reflection (we use pure natural graphite as standard). The X-ray diffraction patterns containing 002 graphite reflection were obtained for all specimens of the functionalized TEGs. The Lorentz function has been selected for approximation of the diffraction peaks.

The qualitative and quantitative composition of the functional groups at the TEG surface was characterized by FTIR spectroscopy. The specimens in a form of pellets 10 mm in diameter were prepared from the powder mixture of TEG and potassium bromide KBr. The experiments were performed on a Perkin Elmer Spectrum BX FTIR spectrometer in the 4000–400 cm^{-1} frequency range.

CMs based on the epoxy resin (ED20) were synthesized by the method described in paper [13] employing the ultrasonication of a liquid epoxy-TEG mixture. The mass fraction of TEG in polymer matrix has been varied from 2 to 8.5 wt.%. In order to prepare TEG/epoxy CMs, TEG were incorporated into epoxy resin ED20 (viscosity of 4000 mPa*s) with polyethylenepolyamine (PEPA) as a hardening agent. To improve the distribution of filler in the polymer matrix, the epoxy was diluted with a small amount of acetone prior to incorporation of GNPs. Then the curing agent PEPA was added and, when the solvent evaporated and the mixtures jellied as the polymerization started, the composite mixture was poured into molds and cured at room temperature. To complete the polymerization, the molds with composite mixtures were exposed to the temperature that gradually increased from 40 to 80°C for 5 hours. Mechanical properties of epoxy resin ED20 and composites based on ED20 are described in paper [14].

For the measurements of electrical conductivity, the samples with shape of rectangular parallelepiped with thickness of 3.5 mm and height of 2.5 mm were prepared. The electrical resistance of CMs was determined by the two-probe (with high resistance values of $>10^7\Omega$) and four-probe (resistance values of $<10^7\Omega$) methods applying direct current at room temperature (this method described in paper [15] in more detail).

To analyze interaction of EMR with CMs the specimens were prepared in a form of 7.2 mm × 3.4 mm × (1.0–1.4) mm plates. Such sample geometry allows for coverage of a section of a rectangular copper waveguide. The scalar network analyzer P2–65 was used to measure the transmission and reflection loss within the 25.5–37.5 GHz frequency range [16]. Voltage measurements of the standing wave ratio were used to determine the reflection properties of the studied specimens [17].

The values of EMR reflection (R), transmission (T) and absorption (A) coefficients, and also the shielding efficiency (SE_T) for the studied CMs were calculated using following relations [18]:

$$R + A + T = 1, \text{ EMR power balance equation,} \tag{1}$$

$$R = |r|^2 = |E_R/E_I|^2,\ T = |t|^2 = |E_T/E_I|^2 \tag{2}$$

$$SE_T = 10\lg(1/T) \tag{3}$$

where E_I,E_R, E_T are the electric field strengths of the incident, reflected and transmitted waves, respectively.

Results and discussion

IR-spectroscopy

Investigations of the produced specimens of thermoexfoliated graphite have been performed using IR-spectroscopy method in order to determine the qualitative and quantitative composition of the functional groups on the surface of functionalized TEG particles. Fig. 1 represents the FTIR absorption spectra of the initial and functionalized TEG powders.

The absorption spectrum for TEG contains a series of peaks and bands, two of which correspond to the impurities, namely, a wide band at 3410 cm^{-1} corresponding to the vibration of the bounded –OH groups (water) and the intensive peak at 2354 Cm^{-1} corresponding to the vibration of carbon dioxide. A group of peaks near 3000 cm^{-1} is observed in the IR spectrum of TEG. They are related to the valency C–H vibrations. Besides, several peaks near 1600 cm^{-1} corresponding to the vibration of C=C and C=O multiple bonds are also observed.

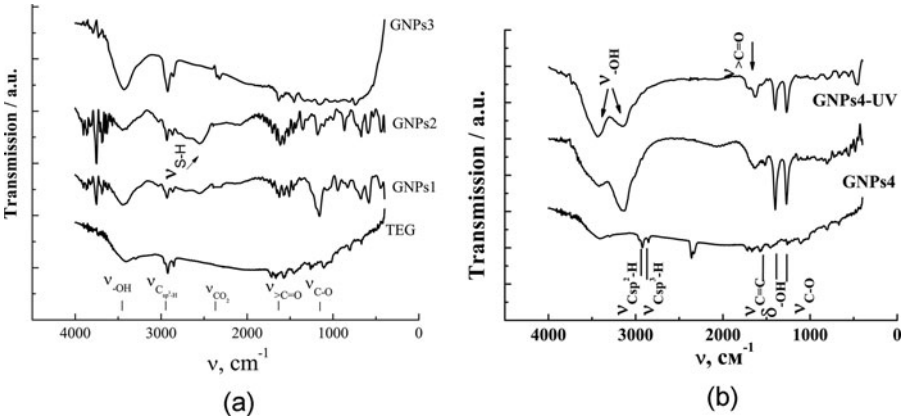

Figure 1. The FTIR spectra of functionalized GNPs: for initial TEG and GNPs after the chemical functionalization – (a); for GNPs after sonication in acetone and UV/ozone treatment – (b).

As well as for the source TEG for all specimens of functionalized TEG the most intensive peaks correspond to the vibration and deformation peaks of O–H groups at 3430 cm^{-1} and peak at 3750 cm^{-1}, which corresponds to the valence vibrations of the hydroxyl –OH group. The intensity of this peak as well as the intensity of peak at 3430 cm^{-1} is significantly higher for the specimens GNPs1, GNPs2. The absorption double peaks observed near 3000 cm^{-1} for all specimens of GNPs and also for the source TEG are conditioned by the hydrogen atoms bonded with sp^2- and sp^3- hybridized carbon atoms. The valency vibrations of C=O double bond cause an intensive signal within 1800–1650 cm^{-1} frequency range for all specimens of the functionalized TEG. A precise position of the carbonyl absorption band at the spectrum depends on the nature of substitutions at C=O carbonyl group. The aromatic C=C stretch and O–H bending give rise to an intense signal at the 1633cm^{-1}. It is strongly marked for the samples of GNPs1,GNPs2, also for these specimens the intensive peaks which are observed at 1560 cm^{-1} 1723 cm^{-1} and correspond to the valency vibrations of C=O and C=C groups are very close to each other and form a broad band. The C–O(epoxy) stretching vibration peak at 1226 cm^{-1}, and the C–O (hydroxyl –OH group.) stretching peak at 1090$cm^{-1}$are observed for GNPs1, GNPs2 specimens, but relative intensity of epoxy and hydroxyl group depends strongly on type of oxidant. A band, which corresponds to the valency vibrations of the lactone group, is observed at 1450 cm^{-1} frequency region. The spectrum region from 1300 cm^{-1} to 625 cm^{-1}, known as "dactylogram" region, contains absorption bands corresponding to the vibrations of C–O group and also to deformation vibrations of $C_{sp}{}^2$-H and C=C groups. A broad absorption band is observed at 2560 cm^{-1}, which is absent at the IR spectrum for the source TEG. This band corresponds to S-H valence vibrations and is conditioned by the presence of the sulfur acid refuses in the functionalized TEG. The intensity if this broad peak is maximal for the specimens GNPs1, GNPs2.

Reasoning from the obtained data, the maximal concentration of hydroxyl group was found for GNPs2. The obtained value essentially exceeds the concentration of hydroxyl group for specimen GNPs1. A substantial value of ketone group concentration was revealed for specimen GNPs2. The concentration of carboxyl and lactone groups for specimen GNPs2 is also the highest; however the difference of concentration in comparison with other specimens is less significant.

It has been found that UV/ozone treatment increases the relative contents of oxygen-containing functional groups on the GNPs surfaces, such as hydroxyl and ether, carboxyl

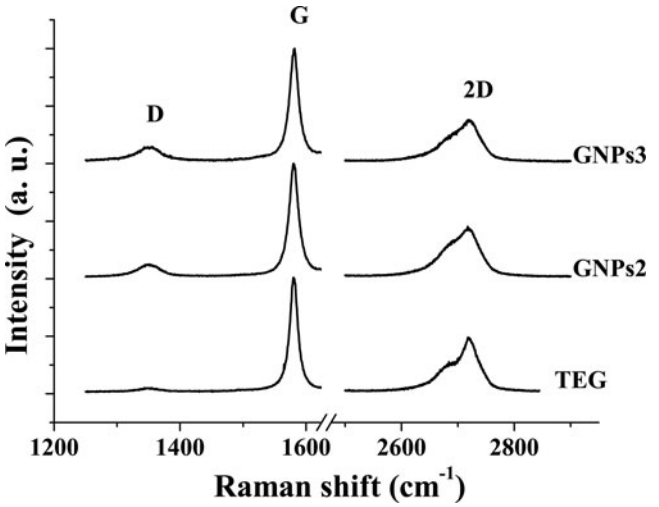

Figure 2. Raman scattering spectra of GNPs.

and carbonyl groups. Changes are observed for GNPs4 sample where the corresponding to stretching vibrations of C=O bond in COOH group appeared quiet distinctly in the absorption band at 1725 cm^{-1}. It should be noted that UV/ozone treatment considerably decreased the intensities of $C_{sp}{}^2$-H band at 2926 $C_M{}^{-1}$ and $C_{sp}{}^3$-H band at 2852 $C_M{}^{-1}$.

It is quite possible that the decrease in $C_{sp}{}^2$-H band intensities at 2926 $C_M{}^{-1}$ and $C_{sp}{}^3$-H band intensities at 2852 $C_M{}^{-1}$ indicates that loosely bonded materials and organic contaminants on the GNPs surface have been removed during the etching process stimulated by ozone. As shown in [11], the UV/ozone treated GNPs also exhibit a rougher surface along with clearer boundaries between the individual basal planes than the untreated graphite does.

Raman spectroscopy

The Raman spectra of initial TEG and functionalized GNPs are shown in Fig. 2. The Raman spectra display three main peaks: the G line, a primary in-plane vibrational mode (~1580 cm^{-1}), 2D (~2700 cm^{-1}), a second order overtone of a different in-plane vibration and the disorder induced D mode (~1350 cm^{-1}). This band is essentially asymmetric for all functionalized graphite specimens with the peculiar "shoulder" at the low-frequency side. The presence of such "shoulder" indicates the presence of the graphite nanoparticles containing low amount of the graphite planes (<10) which was examined in our previous paper [6].

For all the samples D peak is observed. The density of defects was estimated using the model curve obtained for graphene with point deffects [19–21]. Using the semiepiric formula [22]:

$$n_D(\mathrm{cm}^{-2}) = \frac{(1.8 \pm 0.5) \times 10^{22}}{\lambda_L^4} \left(\frac{I_D}{I_G}\right) \tag{4}$$

where λ_L is the excitaiton laser wavelength (in nm), we estimated the defect concentration n_D (in cm^{-2}) (Table 2). The analysis of Raman spectra has shown that as the result of functionalization the defect concentration increases significantly due to reducing the size of the crystallites along the graphite planes. However, after UV/ozone treatment the defect concentration slightly decreases.

Table 2. Values of the broadening (Δh), interlayer distance (d_{002}), crystallite size along *C* axis (L_c) derived from the X-ray diffraction data and defects concentration (n_D) of functionalized GNPs obtained from Raman spectroscopy data of functionalized GNPs.

	X-Ray data				Raman spectroscopy	
Sample	$2\theta.^0$	$\Delta h,^0$	d_{002}, nm	L_c, nm	I_D/I_G	n_D (cm^{-2})
Initial TEG	30.92	0.27	0.3360	40.0	0.03	6.2×10^9
GNPs1	30.87	0.31	0.3364	34.5		
GNPs2	30.92	0.39	0.3363	26.0	0.11	2.4×10^{10}
GNPs3	31.14	0.55	0.3336	18.0	0.12	2.8×10^{10}
GNPs4					0.55	2.6×10^{10}
GNPs4-UV					0.36	1.7×10^{10}

X-Ray diffraction

The structure characterization of functionalized TEG was performed. The values of the interlayer distance and crystallite size for functionalized graphite specimens are presented in Table 2. The results of X-ray analysis have shown that the interlayer distance of all functionalized GNPs doesn't change significantly in comparison to initial TEG and is (0.335 ± 0.001) nm. However, the 002-line broadening is observed and could be related either to decrease of region of X-Rays coherent scattering or to microstresses occurrence on the crystallites edge. The size value of coherent scattering region identified with size of crystallites along *C* axis was calculated according to 002-line broadening data. It was found to be significantly reduced in comparison with initial TEG. This is caused by rupture of Van der Waals bond between graphite planes of initial graphite as a result of chemical and mechanical treatment during functionalization.

Electrical properties

Resistivity measurements were performed to determine the influence of functionalization of GNP on the formation of conductive clusters in CMs. The obtained data are summarized in Table 3.

Previously we demonstrated [12,23] that in the epoxy composite with original (not ultrasonicated) vermicular pristine TEG the percolation threshold (C_{cr}) of electrical conductivity is fairly low ($C_{cr} \sim 0.68$ wt.%). However the main disadvantage of this CM is the high porosity and heterogeneity that makes impossible to obtain the stable shielding characteristics for thin sample (shield). Ultrasonication of TEG in the epoxy-acetone solution leads to defragmentation of the TEG particles. As it was shown the thickness of graphite particles after

Table 3. Characteristics of CMs containing different nanocarbon fillers.

Name	C, wt. %	d,g/Cm^3	P, porosity	$\rho,\Omega\cdot m$	R	A	T	R/A
2TEG	2	0.80	0.34	$7.60\cdot10^{-2}$	0.77	0.221	0.009	3.48
2GNPs1.1	2	1.03	0.15	$1.30\cdot10^{8}$	0.60	0.230	0.170	2.61
5TEG*	5	0.97	0.21	3.43	0.57	0.420	0.010	1.36
5GNPs1.1	5	1.12	0.12	$4.4\cdot10^{7}$			0.106	
5GNPs1.2	5	0.95	0.25	$3.2\cdot10^{7}$			0.93	
5GNPs2	5	1.08	0.12	$3.06\cdot10^{6}$	0.52	0.464	0.016	1.12
5GNPs3	5	0.97	0.21	2.97	0.56	0.400	0.040	1.40
5GNPs4	5	0.98	0.23	$2{,}1\cdot10^{4}$	0.62	0.313	0.067	1.98
5GNPs4-UV	5	0.97	0.24	$8{,}9\cdot10^{2}$	0.568	0.42	0.012	1.36

*Ultrasonicated during 1 hr in acetone medium.

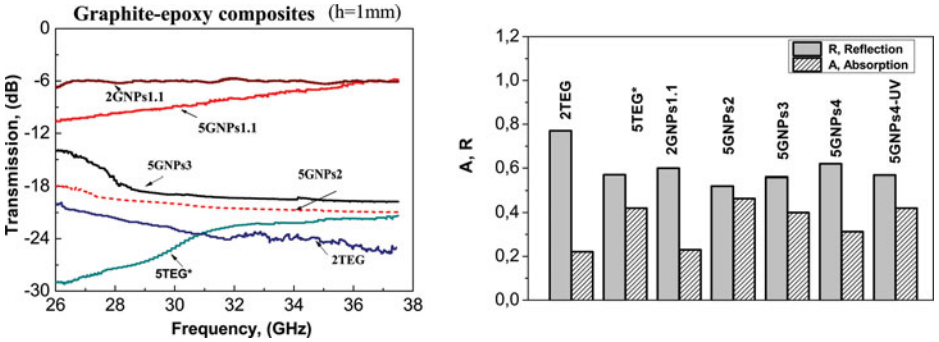

Figure 3. The shielding efficiency SE_T versus EMR frequency of CMs with different types of GNPs – (a), the relation between absorption *A* and reflection *R* indexes of the investigated epoxy CMs –(b).

ultrasonication of TEG in the epoxy-acetone solution during 20 hours is not exceed 5–60 nm. Using of such particles as a fillers allows to obtain the denser and more homogeneous CMs with uniform properties over the entire volume of the sample. But ultrasonication of pristine TEG leads to an increase of C_{cr} up to 6.4 wt.% and widening of the percolation transition in CM [24]. So, the dispersion of TEG to graphite nanoplates leads to worsening of the CM electrical properties. This shift to higher C_{cr} value of the graphite content was explained to be caused by the breakup of the worm-like structure of the TEG particles (i.e., the already formed fragments of graphite clusters) during ultrasonication of TEG in epoxy [13].

Chemical functionalization of pristine TEG nanoparticles changes the properties of the TEG particle surface, creates conditions for uniform distribution of graphite particles in polymer and provides the improved filler–polymer interfacial interaction (enhanced mechanical properties. But it can also worse the electrical and the electrodynamic properties of CM due to destruction of TEG cluster structure. That is why it is necessary to find the optimum between the enhancing of homogeneity in distribution of graphite filler in CMs and partial deterioration of its electrical properties.

The various types of TEG functionalization in combination with ultrasonic dispersion leads to the non-trivial changes in the specific resistance of CMs. In case of GNPs3 the essential changes of electrical properties are not observed due to the fact that in case of this functionalization type (impregnation with ethanol) significant alteration of initial TEG structure also is not observed. While the use of strong oxidants (type 1 and 2 functionalization) leads to a significant increase of the specific resistance of samples. As one can see from Table 3, the specific resistance of CMs containing 2–5 wt.% of functionalized GNPs is significantly (up to 7 orders of magnitude) higher than that in CMs with pristine TEG. The decrease of CMs electrical conductivity could be caused by several reasons: (1) - the loss of the TEG frame structure during functionalization and formation of nanographite particles of form which is strongly depended on the type of oxidant; (2) – during the treatment of carbon material with strong oxidant the destruction of delocalized π-electron system of graphite layer and a partial rupture of σ-bond in graphite layer occur, a substantial number of defects on the nanocarbon surface and deterioration of charge transfer properties, including electric transport properties can be observed [25].

Figure 3 shows the EMR shielding effectiveness over the frequency range of 25–37 GHz for composites with fillers of various types. As one can see, in the CMs with original vermicular pristine TEG filler (such as TEG samples) the shielding efficiency is rater high and for composites containing 2 wt% TEG is measured to be 20–25 dB over the frequency range of

25–37 GHz. It is much more (3–6 times)compared to the shielding efficiency of CM with nanoTEG as well as in the CMs with TEG functionalized by the mixture of sulfur and nitric acids. This is primarily due to the worsening of the electrical properties of CMs with initial TEG compared to the CMs with dispersed TEG. High electrical conductivity of a material usually gives rise to better shielding properties due to enhanced reflection and absorption of electromagnetic waves. But, as it was mentioned above, such CMs are highly inhomogeneous and it is impossible to forecast the electrodynamic properties of specimens with different thickness, especially for thin specimens (shields).

In order to ascertain the influence of functionalization on the formation of conductive clusters in CMs and, correspondingly, on electrical and shielding characteristics the preliminary investigations of the resistivity and measurements of the transmission and reflection loss within the 25.5–37.5 GHz frequency range have been performed for the fabricated GNPs-ED20 composites. The obtained data are summarized in Table 3.

As it is seen from Table 3 the chemical functionalization of TEG particles improved the homogeneity of composite, but the electrical resistivity of composites containing 2–5 wt% of the functionalized TEG is significantly higher (by 4–5 orders) as compare to those with non-functionalized TEG that was not subjected to US dispersing (TEG cluster structure preserved). This is connected with the destruction (under mixing processes) of frame structure of TEG during functionalization, however, the dispersing of TEG allows to fabricate CMs with more uniform bulk distribution of carbon filler. In order to reveal the influence of functionalization on the character of the interfacial interaction and electric characteristics of CMs it is necessary to compare CMs containing graphite filler with the same level of dispersity and concentration. It may be concluded that the various type of TEG functionalization in combination with dispersing (mechanical or ultrasonic) leads to non-trivial changes in electrical resistivity and the shielding efficiency. Fig. 3b schematically presents the relation between A and R for the investigated specimens. A comparison of shielding characteristics for the filler concentration of 5 wt. % can be carried out only with the TEG which has been treated by ultrasound. It is connected with the fact that at such content of unbroken TEG in epoxy matrix the transmission coefficient T is less than 0.001.

As it is seen from Fig. 3b, the shielding due to reflection process (R index) is higher as compared with shielding due absorption (A index) for the all investigated specimens. It was found that functionalization of initial TEG leads to decrease of R index and increase the EMR absorption (A index) in composites with GNPs. However, the dispersing or functionalization of TEG leads to decrease of total shielding efficiency SE_T of CMs with the same filler content. Comparing the values of shielding efficiency (Figs. 3, 4) with data on electrical resistivity (Table 2) it may be concluded that SE_T and reflection index R is proportional to the electrical conductivity.

From Table 3 it can be seen that the major contribution for EMR SE_T comes from the reflection; which is consistent with the literature for nanocarbon composites [12, 23]. As one can see, the shielding efficiency in the above CMs essentially depends on the graphitic filler content.

The dispersion of TEG down to graphite nanoplates leads not only to worsening the CM electrical properties but to increasing the relative contribution of reflection to the shielding efficiency. This is primarily due to the enhanced electrical properties of CMs with initial TEG compared to the CMs with dispersed and functionalized TEG. High electrical conductivity of a material usually gives rise to better shielding properties due to enhanced reflection and absorption of electromagnetic waves. But, as it was mentioned above, such CMs are highly inhomogeneous and it is impossible to determine authentically the dielectric permittivity

$\varepsilon_r^{/}$and dielectric tangent loss tan $\delta$and forecast the electrodynamic properties of specimens with different thickness, especially for thin specimens (shields).

Deterioration of the electrical properties of CMs with dispersed and functionalized TEG (especially for GNPs1 and GNPs2 samples) leads to worsening their shielding characteristics, yet they are stable throughout the volume due to the homogeneity of the specimens. It is also important to note that the shielding efficiency of the CMs mainly increases with increasing the content of carbon nanofiller. Moreover, we can see that the shielding efficiency of the CMs with functionalized TEG slightly deviates from the linear dependence in the region of EMR frequency from 25.5 to 37.5 GHz.

Conclusion

The dispersion and homogeneity of epoxy composites with functionalized thermoexfoliated graphite were improved due to enhancing filler–polymer interfacial interaction (enhanced mechanical properties). The homogeneity of developed composites provides the stable physical characteristics throughout the volume. On the other hand it was found that functionalization in combination with dispersing (mechanical or ultrasonic) of TEG leads to deterioration of electrical and shielding properties of these CMs in comparison with inhomogeneous CMs filled with non-functionalized vermicular TEG. It may be explained by the breaking down the worm-like structure of TEG particles (i.e., the already formed fragments of graphite clusters) during the functionalization and ultrasonic dispersing of TEG in epoxy matrix and increase of percolation threshold. The value of shielding efficiency SE_T is proportional to electrical conductivity of CMs and increases with increase of graphite conductive component content. It was found that functionalization of initial TEG leads to decrease of R index and increase the EMR absorption (A index) in composites with GNPs. The development of such type shielding materials requires finding the optimum between the enhancing of homogeneity in distribution of graphite filler in CMs and partial deterioration of its electrical properties.

References

[1] Plyushch, A., Macutkevic, J., Kuzhir, P. et al. (2016). *Composites Science and Technology*, *128*, 75.
[2] Bychanok, D., Kuzhir, P., Maksimenko, S. et al. (2013). *J. Appl. Phys.*, *113* (12), 124103.
[3] Yadav, S. K., & Cho, J. W. (2013). *Appl. Surf. Sci.*, *266*, 360.
[4] De Bellis, G., Tamburrano, A., & Dinescu, A. et al. (2011). *Carbon*, *49* (13), 4291.
[5] Georgakilas, V., Otyepka, M., Bourlinos, & A. B. et al. (2012). *Chemical reviews*, *112* (11), 6156.
[6] Ovsiienko, I., Lazarenko, O., & Matzui, L. et al. (2014). *physica status solidi*, *211* (12), 2765.
[7] Georgakilas, V., Tiwari, J. N., Kemp, & K. C. et al. (2016). *Chemical reviews*, *116* (9), 5464.
[8] Wang, Y., Yang, C., Mai, & Y.-W. et al. (2016). *Carbon*, *102*, 311.
[9] Kim, J.-H. and Min, & B.-G. (2010). *Carbon letters*, *11* (4), 298.
[10] Simmons, J. M., Nichols, B. M., Baker, & S. E. et al. (2006). *The Journal of Physical Chemistry B*, *110* (14), 7113.
[11] Li, J., Kim, J.-K., and Lung Sham, & M. (2005). *Scr. Mater.*, *53* (2), 235.
[12] Lazarenko, O., Vovchenko, L., & Matzui, L. et al. (2011). *Mol. Cryst. Liq. Cryst.*, *536* (1), 72/[304].
[13] Lazarenko, A., Vovchenko, L., & Matsui, D. et al. (2008). *Mol. Cryst. Liq. Cryst.*, *497* (1), 65/[397].
[14] Vovchenko, L., Lazarenko, O., & Matzui, L. et al. (2014). *physica status solidi*, *211* (2), 336.
[15] Perets, Y. S., Matzui, L. Y., & Vovchenko, L. L. et al. (2014). *J. Mater. Sci.*, *49* (5), 2098.
[16] Vovchenko, L., Matzui, L., & Oliynyk, V. et al. (2008). *Mol. Cryst. Liq. Cryst.*, *497* (1), 46/[378].
[17] Harvey, A. F. *Microwave engineering* (Academic Press, 1963).
[18] Al-Saleh, M. H., & Sundararaj, U. (2009). *Carbon*, *47* (7), 1738.
[19] Lucchese, M. M., Stavale, F., Ferreira, & E. H. M. et al. (2010). *Carbon*, *48* (5), 1592.

[20] Martins Ferreira, E. H., Moutinho, M. V. O., & Stavale, F. et al. (2010). *Physical Review B*, *82* (12), 125429.
[21] Szroeder, P., Górska, A., & Tsierkezos, N. et al. (2013). *Materialwissenschaft und Werkstofftechnik*, *44* (2–3), 226.
[22] Cançado, L. G., Jorio, A., & Ferreira, E. H. M. et al. (2011). *Nano Lett.*, *11* (8), 3190.
[23] Vovchenko, L., Matzui, L., & Oliynyk, V. et al. (2010). *physica status solidi*, *7* (3–4), 1260.
[24] Vovchenko, L. L., Matzui, L. Y., & Oliynyk, V. V. et al. (2011). *Mol. Cryst. Liq. Cryst.*, *535* (1), 179.
[25] Stankovich, S., Dikin, D. A., & Piner, R. D. et al. (2007). *Carbon*, *45* (7), 1558.